2-7-2021

Analysis of Side Coupled Microstrip Filters Using Three Dimensional FDTD with Berenger Perfectly Matched Layer (PML).

Maher Abd Elrazzak

Member, IEEE Faculty of Eng., Mansoura Univ., Mansoura, Egypt., maher@mum.mans.enu.eg

Follow this and additional works at: https://mej.researchcommons.org/home

Analysis of Side Coupled Microstrip Filters Using Three Dimensional FDTD with Berenger Perfectly Matched Layer (PML)

تحليل المرشحات الشريطية المترابطة جانبيا باستخدام طريقة الفروق المحدودة فى
الاطار الزمنى ذات الثلاث أبعاد مع الطبقات المتوائمة تماما لبرنجر

Maher M. Abd Elrazzak, *Member, IEEE*
Faculty of Eng., Mansoura Univ., Mansoura, Egypt.
email: maher@mum.mans.enu.eg

فى هذا البحث تم استخدام طريقة الفروق المحدودة فى الحيز الزمنى ذى الثلاثــة
أبعاد (Finite difference time domain) مع الطبقات تامة المواءمة لبرنجر(Breneger PML) فى
تحليل المرشحات الشريطية المترابطة جانبيا. وتم دراسة تأثير سمك تلك الطبقات المتوائمة تماما فى هذا التحليـــل. و
لهذه المرشحات تم حساب المجالات فى الحيز الزمنى (Timer domain field response) .
بارامترات التبعثر(Scattering parameters)، و معاوقة الدخل (Input impedance). وقد وجدنـــا
تحسننا ملحوظا لهذه الطريقة على الطرق المنشوره كطريقة الفروق المحدودة فى الاطــار الزمنـــى ذات الثـــلاث
أبعاد مع الشروط الحدية الممتصة لمير (Mur ABCs) و طريقة الدوائر المكافئه للمرشح

Abstract- In this paper, the finite difference time domain technique with the Berenger's perfectly matched layer (PML) is applied for the analysis of side coupled microstrip filters. The effect of the PML thickness is studied. Numerical results for the time domain response, the scattering parameters, and the input impedance are obtained. Good improvement of the present results over that published and obtained by FDTD method with the Mur's absorbing boundary condition or that obtained by the equivalent circuit model method are found.

1. Introduction

The finite difference time-domain method has become one of the most widely used technique of electromagnetic scattering, radiation, and propagation problems. One of the advantages of the FDTD is that the analysis is stable and yields a unique result while the frequency-domain analysis suffers from spurious solutions. The method is based on the discretizatioo of the differential form of Maxwell's equations in the time and space domains using second order accurate central differences. The obtained difference equations are then solved in a time marching sequence for calculating both the electric and magnetic fields on an interlaced cartesian grid[1-3]. The use of the FDTD in electromagnetics requires the use of radiation or absorbing boundary conditions (ABCs) to minimize the discretization " computational" domain [4-6]. During the last few decades, a number of ABCs have been proposed. These include Mur ABCs [4-5] in which the outgoing wave equation is approximated by linear expressions using either a Taylor or Pade approximation. Other ABCs have been proposed and are summarized in [1,6]. Recently, Breneger introduced ABC named Perfectly Matched Layer (PML)[7-9]. PML is a nonphysical absorber adjacent

to the outer computational boundary. The PML ensures that the out-going fields of arbitrary frequency and incident angle are absorbed in the PML region with negligible reflections toward the inner structure.

In the present work, the FDTD method with the Berenger PML is used for the analysis of side coupled microstrip filters. The time domain and the frequency domain characteristics are obtained. The frequency characteristics are calculated using a cosine pulse and applying the Fourier transform to the transient response of the circuit. This leads to obtain the frequency characteristics over the full range of frequencies simultaneously.

In the next sections, we will give the basic mathematical formulation of both the FDTD and the PML. The analysis of the microstrip filters is described in section III with its numerical results. Finally, the concluding remarks are given in section IV.

II. Formulation of the Problem
A. Time Domain Finite Difference formulation

The microstrip transmission line filter is shown in Fig. 1 where the strips and the bottom planes are made of perfectly conducting material. The substrate has a relative dielectric constant ε_r. The microstrip line is taken as an open structure. For this structure, Maxwell's equations can be written as:
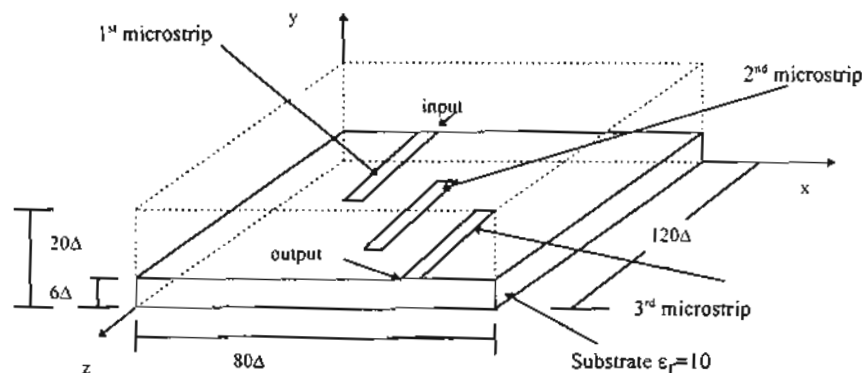

Fig. 1 The side-coupled microstrip filter configuration (the spaces between the strips and the strip widths are 6Δ and centered on the substrate)

$$\frac{\partial \overline{H}_i}{\partial t} = -\frac{1}{\mu_i}\nabla \times \overline{E}_i - \frac{\rho_i}{\mu_i}\overline{H}_i \tag{1.1}$$

$$\frac{\partial \overline{E}_i}{\partial t} = \frac{1}{\varepsilon_i}\nabla \times \overline{H}_i - \frac{\sigma_i}{\varepsilon_i}\overline{E}_i \tag{1.2}$$

where,

ρ : is the magnetic resistivity of the medium in (Ω/m)

σ : is the electric conductivity of the medium in (S/m)

i=1.2 represents the substrates and free space, as shown in the Fig.1.

To discretize Maxwell's equations (1), the centered difference approximation is applied to both time and space first-order partial differentiations. Following Yee [10], one can arrange the spatial nodal points where different components of E and H are to be determined, as shown in Fig. 2. This leads to the discretized Maxwell's equations for homogeneous regions as follows [1]:

$$H_x\Big|_{i,j,k}^{n+1/2} = D_a\Big|_{i,j,k} \cdot H_x\Big|_{i,j,k}^{n-1/2} +$$

$$D_b\Big|_{i,j,k} \left\{ \frac{E_y\Big|_{i,j,k+1/2}^{n} - E_y\Big|_{i,j,k-1/2}^{n}}{\Delta z} - \frac{E_z\Big|_{i,j+1/2,k}^{n} - E_z\Big|_{i,j-1/2,k}^{n}}{\Delta y} \right\} \quad (2.1)$$

$$H_y\Big|_{i,j,k}^{n-1/2} = D_a\Big|_{i,j,k} \cdot H_y\Big|_{i,j,k}^{n-1/2} +$$

$$D_b\Big|_{i,j,k} \cdot \left\{ \frac{E_z\Big|_{i+1/2,j,k}^{n} - E_z\Big|_{i-1/2,j,k}^{n}}{\Delta x} - \frac{E_x\Big|_{i,j,k+1/2}^{n} - E_x\Big|_{i,j,k-1/2}^{n}}{\Delta z} \right\} \quad (2.2)$$

$$H_z\Big|_{i,j,k}^{n+1/2} = D_a\Big|_{i,j,k} \cdot H_z\Big|_{i,j,k}^{n-1/2} +$$

$$D_b\Big|_{i,j,k} \cdot \left\{ \frac{E_x\Big|_{i,j+1/2,k}^{n} - E_x\Big|_{i,j-1/2,k}^{n}}{\Delta y} - \frac{E_y\Big|_{i+1/2,j,k}^{n} - E_y\Big|_{i-1/2,j,k}^{n}}{\Delta x} \right\} \quad (2.3)$$

$$E_x\Big|_{i,j,k}^{n+1} = C_a\Big|_{i,j,k} \cdot E_x\Big|_{i,j,k}^{n} +$$

$$C_b\Big|_{i,j,k} \left\{ \frac{H_z\Big|_{i,j+1/2,k}^{n+1/2} - H_z\Big|_{i,j-1/2,k}^{n+1/2}}{\Delta y} - \frac{H_y\Big|_{i,j,k+1/2}^{n+1/2} - H_y\Big|_{i,j,k-1/2}^{n+1/2}}{\Delta z} \right\} \quad (2.4)$$

$$E_y\Big|_{i,j,k}^{n+1} = C_a\Big|_{i,j,k} \cdot E_y\Big|_{i,j,k}^{n} +$$

$$C_b\Big|_{i,j,k} \left\{ \frac{H_x\Big|_{i,j,k+1/2}^{n+1/2} - H_x\Big|_{i,j,k-1/2}^{n+1/2}}{\Delta z} - \frac{H_z\Big|_{i+1/2,j,k}^{n+1/2} - H_z\Big|_{i-1/2,j,k}^{n+1/2}}{\Delta x} \right\} \quad (2.5)$$

$$E_z\Big|_{i,j,k}^{n+1} = C_a\Big|_{i,j,k} \cdot E_z\Big|_{i,j,k}^{n} +$$

$$C_b\Big|_{i,j,k} \left\{ \frac{H_y\Big|_{i+1/2,j,k}^{n+1/2} - H_y\Big|_{i-1/2,j,k}^{n+1/2}}{\Delta x} - \frac{H_x\Big|_{i,j+1/2,k}^{n+1/2} - H_x\Big|_{i,j-1/2,k}^{n+1/2}}{\Delta y} \right\} \quad (2.6)$$

where Δx, Δy, and Δz are the space discretization units in the x, y, and z directions, respectively. The C's and D's coefficients are as given in reference [1].
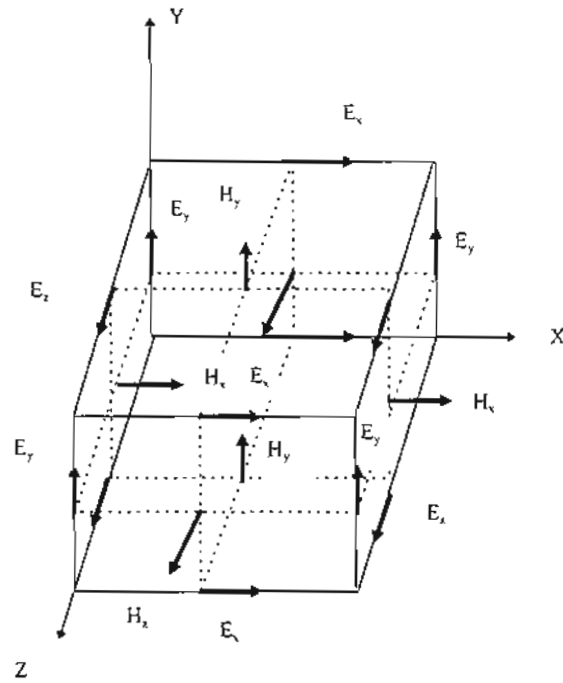
Fig. 2 The position of the electric and magnetic field

components in the Yee's FDTD cell

For a non-homogeneous domain, each homogeneous region is treated separately and then the boundary conditions are forced at the interfaces.

To ensure that the numerical error generated in one calculation step does not accumulate and grow, the stability criterion of Yee's algorithm relates Δ_x, Δ_y, and Δ_z and Δt is applied [1],

$$\Delta t \le \frac{1}{V_c} \left(\frac{1}{\Delta x^2} + \frac{1}{\Delta y^2} + \frac{1}{\Delta z^2} \right)^{-\frac{1}{2}} \tag{3}$$

where

Δt is the maximum time step that may be used, and

V_c is the velocity of light

B. Perfectly Matched Layer PML

The PML is a nonphysical absorber adjacent to the outer boundary of the open structure computational domain. The PML ensures that a plane wave incident at any arbitrary angle or frequency from the free-space upon a PML region is totally transmitted into PLM region with a negligible reflections toward the inner structure [7,8]; i.e. total absorption for the outgoing waves. This is carried out by introducing an additional degree of freedom by splitting the field components with anisotropic

material properties in the PML region. For this material, the electric conductivity and the magnetic loss is related by [7],

$$\frac{\sigma}{\varepsilon_o} = \frac{\sigma^{\cdot}}{\mu_o} \tag{4}$$

where $\sigma^{\cdot}$ denotes the magnetic conductivity.

Theoretically, for a layer of such conductivities there is no reflections from the inner sides of the PML region to the inner structure (computational domain). However, the outgoing waves are reflected by the perfectly conducting conditions at the outer boundary of the PML region and may be returned to the inner domain. Berenger [7] suggested a conductivity profile($\sigma(\rho)$); ρ is the distance from the inner interface) which provides the decay of the outgoing field to zero as it goes to the outer boundaries. This eliminates totally reflections from the outer boundary of the PML to the inner structure. Accordingly, Maxwell's equations can be written as [11],

$$\mu_o \frac{\partial H_{xy}}{\partial t} + \sigma_y^{'} H_{xy} = -\frac{\partial \left(E_{zx} + E_{zy} \right)}{\partial y} \tag{5.1.a}$$

$$\mu_o \frac{\partial H_{xz}}{\partial t} + \sigma_z^{\cdot} H_{xz} = \frac{\partial \left(E_{yx} + E_{yz} \right)}{\partial z} \tag{5.1.b}$$

$$\mu_o \frac{\partial H_{yz}}{\partial t} + \sigma_z^{\cdot} H_{yz} = -\frac{\partial \left(E_{xy} + E_{xz} \right)}{\partial z} \tag{5.2.a}$$

$$\mu_o \frac{\partial H_{yx}}{\partial t} + \sigma_x^{\cdot} H_{yx} = \frac{\partial \left(E_{zx} + E_{zy} \right)}{\partial x} \tag{5.2.b}$$

$$\mu_o \frac{\partial H_{zx}}{\partial t} + \sigma_x^{\cdot} H_{zx} = -\frac{\partial \left(E_{yx} + E_{yz} \right)}{\partial x} \tag{5.3.a}$$

$$\mu_o \frac{\partial H_{zy}}{\partial t} + \sigma_y^{\cdot} H_{zy} = \frac{\partial \left(E_{xy} + E_{xz} \right)}{\partial y} \tag{5.3.b}$$

$$\varepsilon_o \frac{\partial E_{xy}}{\partial t} + \sigma_y E_{xy} = \frac{\partial \left(H_{zx} + H_{zy} \right)}{\partial y} \tag{5.4.a}$$

$$\varepsilon_o \frac{\partial E_{xz}}{\partial t} + \sigma_z E_{xz} = -\frac{\partial \left(H_{yx} + H_{yz} \right)}{\partial z} \tag{5.4.b}$$

$$\varepsilon_o \frac{\partial E_{yz}}{\partial t} + \sigma_z E_{yz} = \frac{\partial \left(H_{xy} + H_{xz} \right)}{\partial z} \tag{5.5.a}$$

$$\varepsilon_o \frac{\partial E_{yx}}{\partial t} + \sigma_x E_{yx} = -\frac{\partial \left(H_{zx} + H_{zy} \right)}{\partial x} \tag{5.5.b}$$

$$\varepsilon_o \frac{\partial E_{zx}}{\partial t} + \sigma_x E_{zx} = \frac{\partial \left(H_{yx} + H_{yz} \right)}{\partial x} \tag{5.6.a}$$

$$\varepsilon_o \frac{\partial E_{zy}}{\partial t} + \sigma_y E_{zy} = -\frac{\partial \left(H_{xy} + H_{xz} \right)}{\partial y} \tag{5.6.b}$$

III. Analysis of Microstrip Filter

The configuration of the analyzed microstrip filter is shown in Fig. 1. The space steps are $\Delta x=\Delta y=\Delta z=0.212$ mm and the total mesh dimensions are 80X20X120 in the x, y, and z directions, respectively. At the top and side faces, a PML of width with different number of cells is considered. The microstrip line parameters are [12]:

width of the microstrip conductor W=6Δ,
thickness of the substrate H=6Δ;
dielectric constant of the substrate ε_r =10.0,and
length of each transmission line =60Δ.

The time step used is Δt=0.176 ps. The input signal is a band-limited cosine pulse of the form,

$$E_y(t) = 1 - \cos(2\pi f_{band} t) \qquad \text{for} \quad 0 \le t \le 1/f_{band}$$
$$= 0 \qquad\qquad\qquad \text{for} \quad t > 1/f_{band}$$
$$f_{band} = 11.8 \text{ GHz}$$

This pulse is fed under the microstrip conductor at the plane z=0, and the initial values of the other components are made zero.

The input pulse is applied to the input port of the first microstrip line and then electromagnetic field is calculated at different time. . The time variation of the E_y component at the x-z plane in the substrate is shown in Fig. 3. The incident signal propagation along the first microstrip is observed; Fig.3 (a) to (c). In Fig. 3(c), the signal arrived to the end of microstrip and reflected to the input port. A part of the wave transferred to the second microstrip line and the reflected wave went back to the input port, Fig. 3 (d) and Fig. 3 (e). In Fig. 3 (f) and Fig. 3(g), the signal resonates around the second microstrip line. In Fig. 3 (h), the resonance component transfers to the third microstrip line and it is transmitted to the output port.

The time variations of electromagnetic field components E_y at different points on the first microstrip is shown in Fig. 4 where the incident and reflected waves are shown. In Fig. 5, the transmitted wave at the output port of the third microstrip line is shown.   From these figures, it can be shown that the incident and reflected waves go to steady state after about 6,000 time steps while the transmitted wave after about 30.000 time steps. By applying the Fourier transform to the incident, refelected, and transmitted waves, one can calculate the S-parameters and the input impedance of the side-coupled filter shown in Fig. 1 [2,5].

Fig. 6, Fig. 7, and Fig. 8 show the S-parameters, the real part, and of the imaginary part of the normalized input impedance. This is carried out considering different number of perfect matched layer (NPML) cells; NPML = 2, 4, 8 cells. Good results are obtained with NPML equal or greater than 4 cells . From   Fig. 7, and Fig. 8, it is observed that at the resonance frequencies the real part of the input impedance makes maximum values while the imaginary part tends to zero.

In Fig. 9, the present S-parameters (for NPML=8) are compared with the available published results [12,13]. In [12], the authors compare their simulated results obtained by the equivalent circuit model of the circuit with an experimental data. In [13], the FDTD with Mur ABCs was used in the analysis. From Fig. 9, it is obvious that the difference between the magnitude of S11 from the different techniques is very small. This is because the calculations of S11 is based on the Fourier transform of the incident and reflected waves in which the computational error is very small; these waves tend to steady state after 6,000 time step. On the other hand, the difference in S21 is shown. This is because S21calculations are based on the transmitted signal at the output port which is sensitive to the reflections at this port and it tends to steady state after 30,000 time steps. The present S-parameters which are based on the PML absorber are in better agreement with the experimental results given in [12], especially at the resonance frequency of 8 GHz than that obtained by either the equivalent circuit model [12] or that of the FDTD with Mur absorbing boundary condition [13].

In the second example, a side coupled microstrip filter with a second microstrip line of length equal 80Δ is considered . The time variation of the E_y component is shown in Fig. 10. It is clear from this figure that a part of the incident wave is transferred to the second microstrip line earlier than the case shown in Fig. 3. In addition, the resonance waves become more concentrated on the second microstrip line while the transferred (transmitted) wave to the third microstrip line, Fig. 10 (h), become less than that shown in Fig. 3 (h).

In Fig.11 and Fig. 12, the incident, refelected, and transmitted waves at different points at the first microstrip and the end of the third microstrip line are shown. It is seen from Fig. 11 that the increasing of the length of the second microstrip line leads to decrease the amplitude of the reflected wave when it is compared with that in Fig. 4. In addition, the transmitted wave in Fig. 11 is also decreased when it is compared with that in Fig. 5.

The scattering parameters and the normalized input impedance are shown in Fig. 13, and Fig14, respectively. These figures show that the resonance frequencies decreases with increasing the length of the second microstrip line.

IV. Conclusion
In the present work, the time domain response, the scattering parameters, and the input impedance of the side coupled-side microstrip filters are studied. This is carried out by using the finite difference time domain method with the Breneger perfect matched layer. One important advantage of the FDTD is that the analysis is stable and yields a unique result while the frequency-domain analysis suffers from spurious solutions. In addition, with the aid of Fourier transform to the transient response of the circuit the frequency characteristics over the full range of frequencies are obtained simultaneously. With Berengers PML, the reflections from the outer boundary of the PML to the inner structure (computational domain) are totally eliminated. This leads to increase the accuracy of the present computations. The effect of changing the PML thickness is considered. The obtained results are compared with the available published data. It has been found that the present results are in

better agreement with the experimental results than these obtained by either the equivalent circuit model or that of the FDTD with Mur absorbing boundary condition.

REFERENCES

[1] Karl. S. Kuenz and Raymound J. Luebbers, The Finite- Difference Time - Domain Method for Electromagnetics CRC press, London Tokyo, 1993.

[2] M. A. Schamberger, S. Kosanovich, and R. Mittra, " Parameter extraction and correction for transmission lines and discontinuities using the finite-difference time-domain method," IEEE Trans., Microwave Theory Tech., vol. MTT-44, No.6, pp.919-925, June 1996.

[3] P. A. Tirkas and C. A. Balanis, " Finite- difference time-domain method for antenna radiation, " IEEE Trans., Antennas Propagat., vol. AP-40, pp. 334-340, March 1992.

[4] Mur G., " Absorbing boundary conditions for the finite-difference approximation of the time-domain. electromagnetic field equations," IEEE Trans., Electromagnetic Compat., vol. 23, no. 4, pp.377 - 382, Nov.1981.

[5] D. M. Sheen, S. M. Ali, M. D. Abouzahra, and J. A.Kong, "Application of the three - dimensional finite - difference time-domain method to the analysis of planar microstrip circuits, " IEEE Trans., Microwave Theory Tech., vol . MTT-38. No. 7, pp.849-857, July. 1990.

[6] W. V. Andrew, C, A. Balanis, and P. A. Trikas, " a comparison of the Breneger perfect matched layer and the Lindman higher order ABC's for the FDTD method." IEEE Microwave and Guided Wave Letters vol. 5, No. 6, pp. 192-194. June1995.

[7] Jean -Pierre Berenger. " A perfectly matched layers for the FDTD solution of wave-structure interaction proplems," Trans., Antenna and Propagat., vol. AP-44, No. 1, pp.110-117, Jan. 1996.

[8] B. Chen. D. J. Fang and B. H. Zhou. "Modified Berenger PML absorbing boundary conditions for the FD- TD meshes," IEEE Microwave and Guided Wave Letters vol.5, no.11, Nov.1995.

[9] D.T. Aescoh, and N. V. Shuley, " Reflection analysis of FDTD boundary conditions-Part II: Breneger's PML absorbing layers," IEEE Trans., Microwave Theory Tech., vol. MTT-45, No. 8, pp.1171-1175, Aug. 1997.

[10] K. S. Yee, " Numerical solution of initial boundary value problems involving Maxwell's equations in isotropic media," IEEE Trans. Antennas Propagat., vol. AP-14, pp. 302-307; May 1966.

[11] R. Mittra, and U. Pekel, " A new look at the perfect matched layer (PML) concept for the reflectionless absorption of electromagnetic waves," IEEE Microwave and Guided Wave Letters vol.5, no.3, pp. 84-86, march 1995.

[12] T. S. Hibata, and T. Hayashi and T. Kimura, " Analysis of microstrip circuits using three dimensional full -wave electromagnetic field analysis in the time domain," IEEE Trans. Microwave theory Tech., vol. 36, no. 6, pp.1064-1070, June 1988.

[13] C. J. Railton, Elizabeth M. Daniel, Dominique-Lynda Paul, and Joseph P. Mc Geehan, "Optimized absorbing boundary conditions for the analysis of planar circuits using finite-difference time-domain method," IEEE Trans., Microwave Theory Tech., vol. MTT-41, no.2, pp.290-297, Feb.1993.
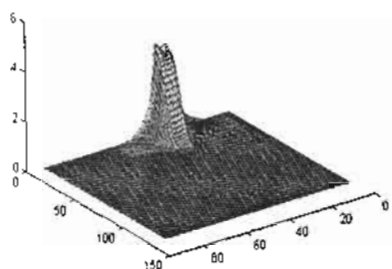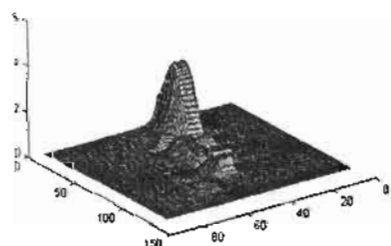
(a) t=300
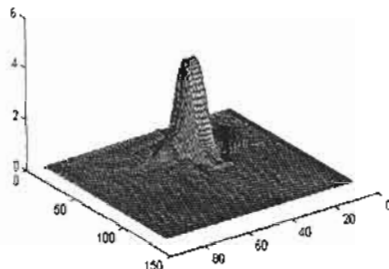
(b) t=600
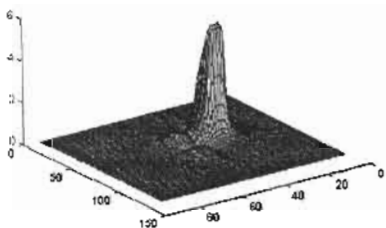
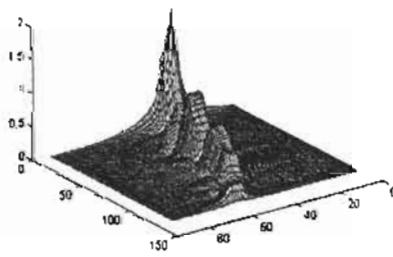(c) t=900
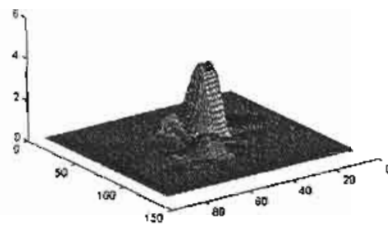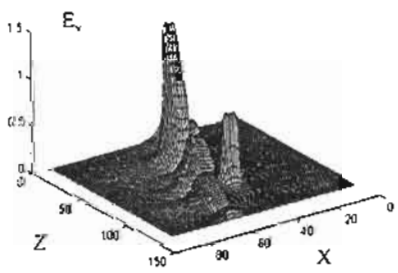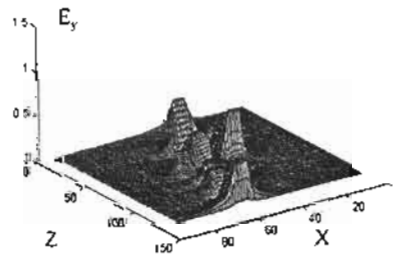
(d) t=1200

(e) t=1500

(f) t=1800

(g) t=2100

(h) t=2400

Fig. 3 The time variation of the electric field component E_y at the x-z plane in the substrate
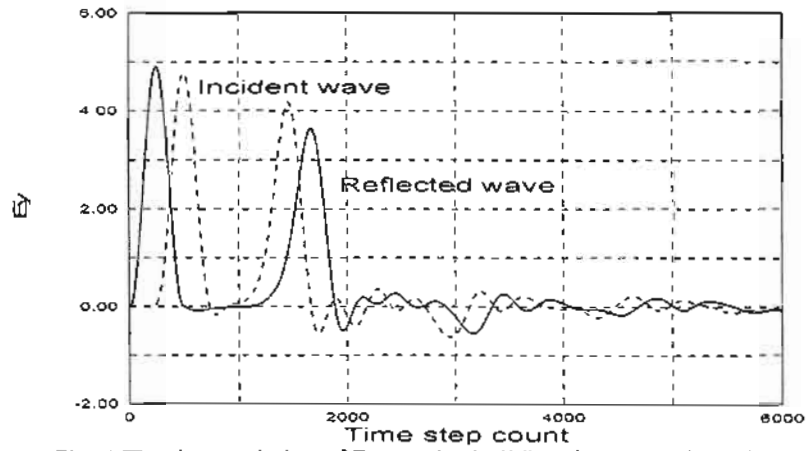
Fig. 4 The time variation of E_y at $z=1\Delta$ (solid) and $z=20\ \Delta$ (dashed)
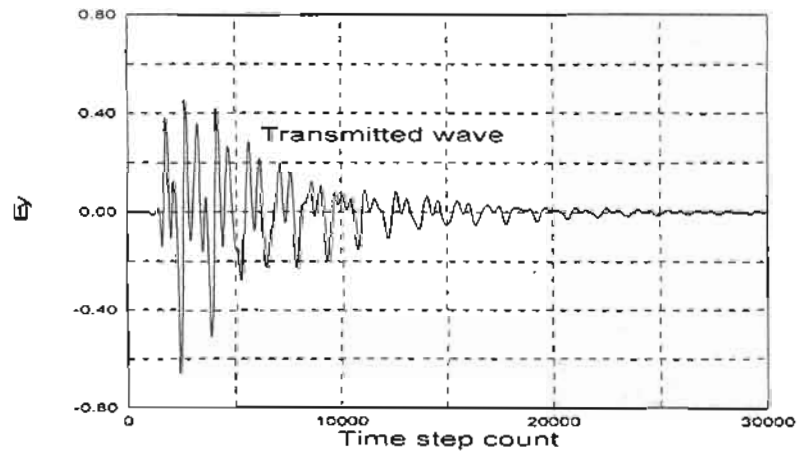

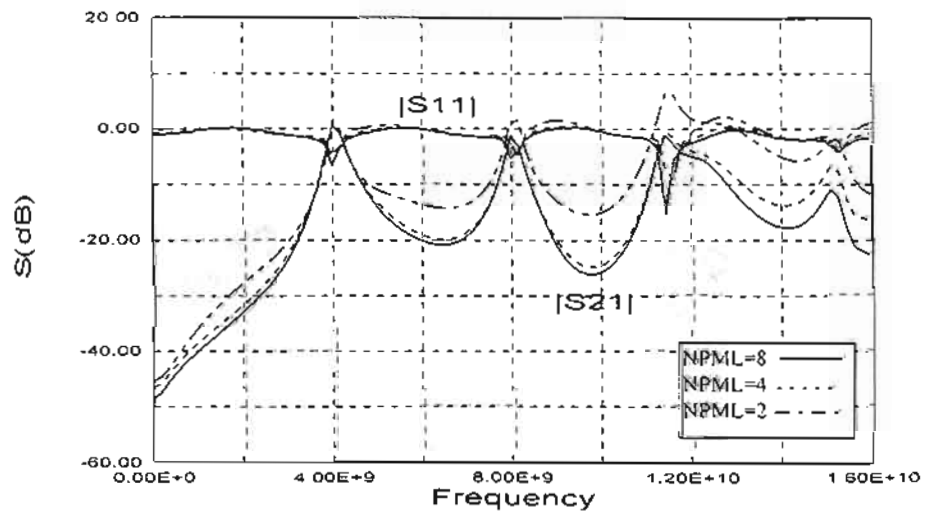Fig. 5 The time variation of E_y at the output port
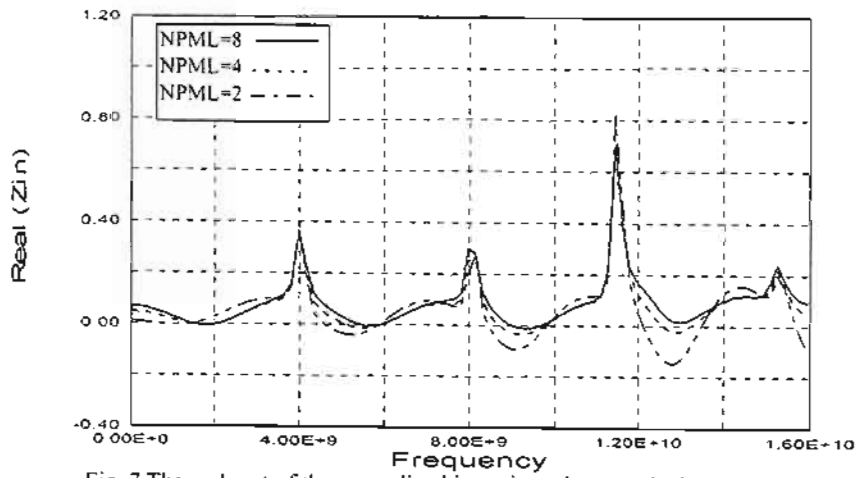

Fig. 6 The scattering parameters $|S11|$ and $|S21|$

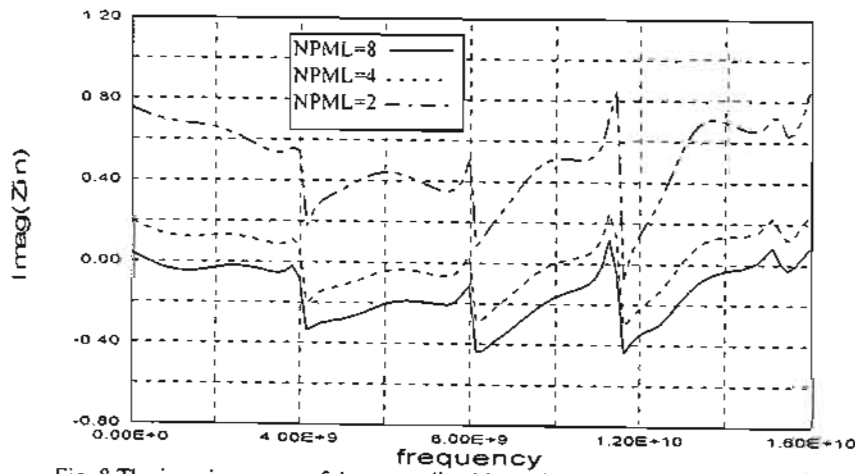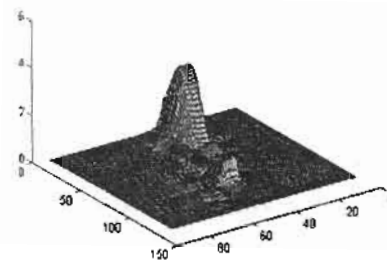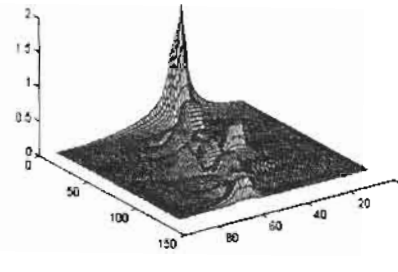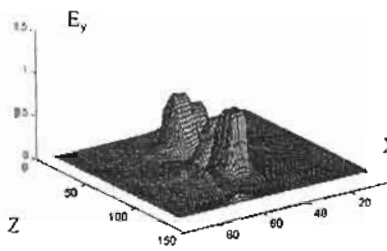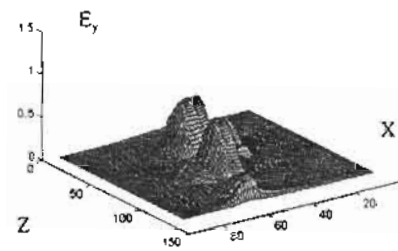Fig. 7 The real part of the normalized input impedance at the input port

Fig. 8 The imaginary part of the normalized input impedance at the input port
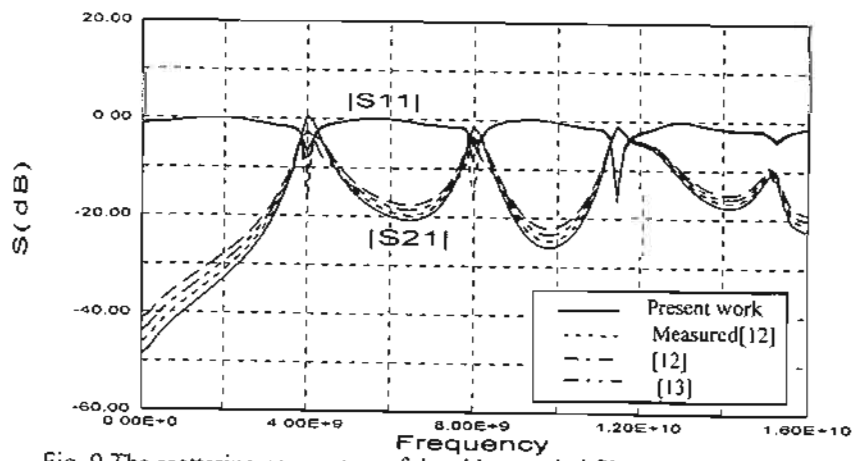
Fig. 9 The scattering parameters of the side-coupled filter shown in Fig. 1
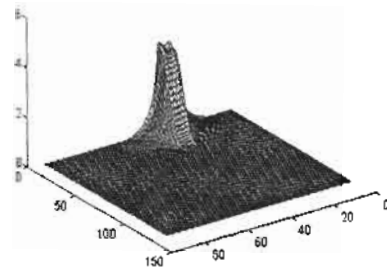
(a) t=300
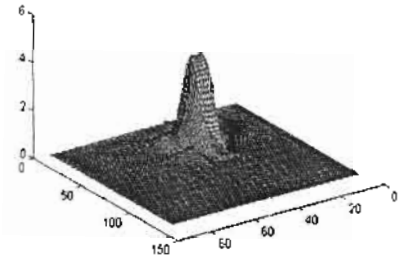
(b) t=600
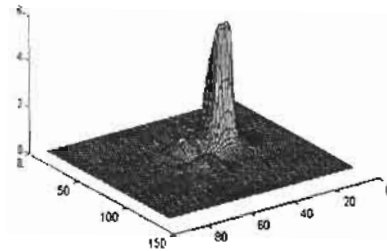
(c) t=900
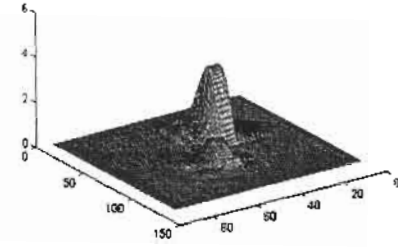
(d) t=1200

(e) t=1500

(f) t=1800

(g) t=2100

(h) t=2400

Fig. 10 The time variation of the electric field component E_y at the x-z plane in the substrate with the second microstrip line has the length of 80 Δ
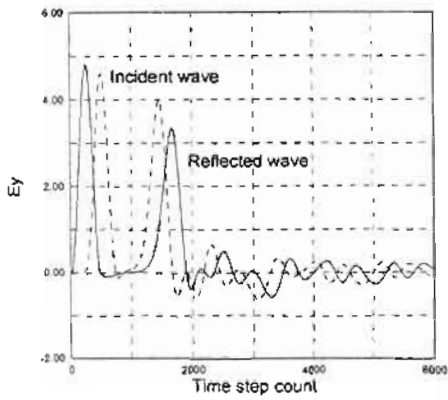
Fig. 11 The time variation of E_y at $z=1\Delta$ (solid) and $z=20\Delta$ (dashed) with the second microstrip has length equal 80 Δ
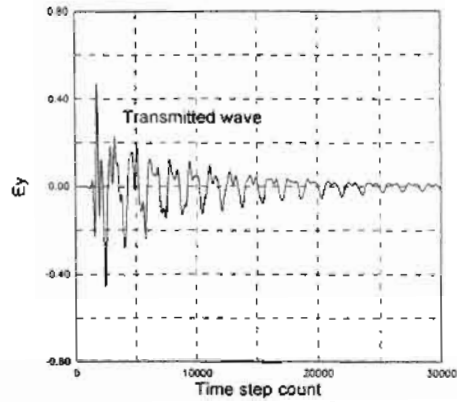

Fig. 12 The time variation of E_y at the output port with the second microstrip has length equal 80 Δ
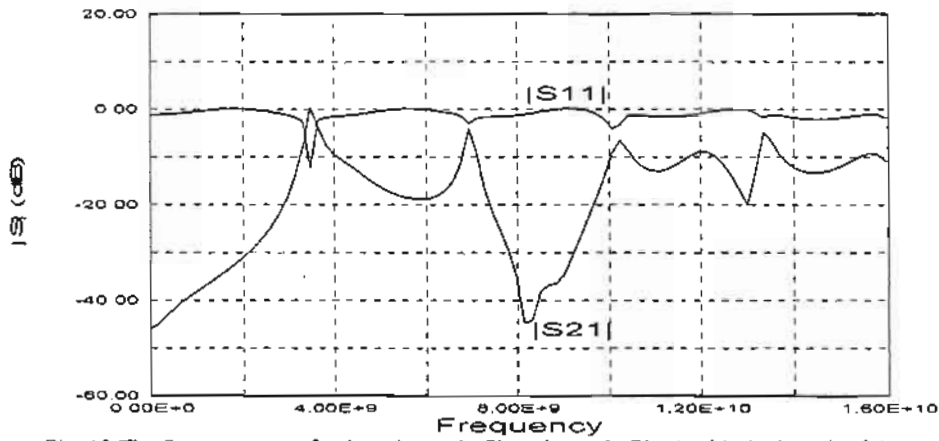

Fig. 13 The S-parameters of the microstrip filter shown in Fig. 1 with the length of the second microstrip line equal 80 Δ
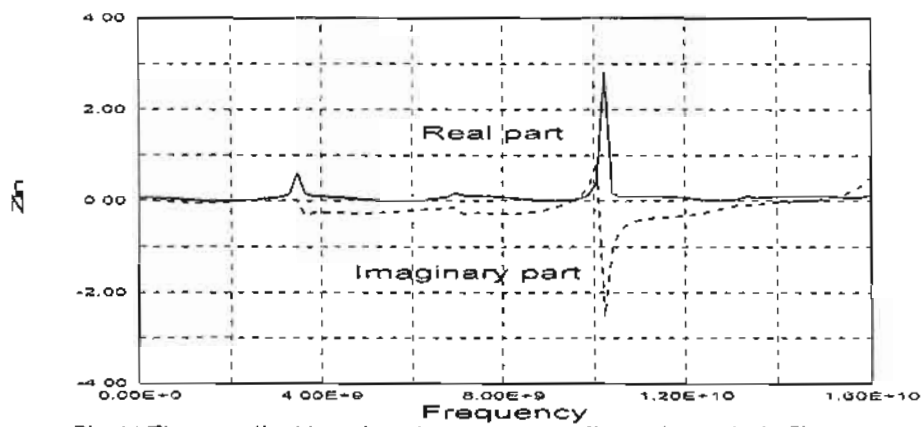

Fig. 14 The normalized input impedance corresponding to the results in Fig. 12